Xenon as a transdermal enhancer for niacinamide in Strat-M™ membranes

Evgeny Petrov*, Alexander Verkhovskiy
Laboratory of Biochemistry of Transport Systems, Faculty of Innovative Technologies, National Research Tomsk State University, Tomsk, Russian Federation

*Correspondence to: Evgeny Petrov, PhD, petrov67@gmail.com.
orcid: 0000-0002-4055-6981 (Evgeny Petrov)

Abstract

Xenon is confirmed to diffuse readily through membranes and has properties of transdermal enhancer. In this study, the ability of xenon to regulate the transdermal diffusion of niacinamide was investigated using a model of an artificial skin analogue of Strat-M™ membranes in Franz cells. Based on the data obtained, we found that in the simplified biophysical model of Strat-M™ membranes xenon exerts its enhancer effect based on the heterogeneous nucleation of xenon at the interfaces in the microporous structures of Strat-M™ membranes.

Key words: enhancer; Franz cell; gas nucleation; niacinamide; permeation; skin; Strat-M; transdermal drug delivery system; xenon

doi: 10.4103/2045-9912.320704
How to cite this article: Petrov E, Verkhovskiy A. Xenon as a transdermal enhancer for niacinamide in Strat-M™ membranes. Med Gas Res. 2022;12(1):24-27.
Funding: This work was supported by the Xenon Skincare International, Inc. (East Stroudsburg, PA, USA), represented by Dr. Mikhail Artamonov.

Introduction

Xenon is an inert gas with a number of interesting biologically active properties. Detailed studies have shown that xenon atoms are localized in hydrophobic "pockets" of protein molecules – small cavities with predominantly short hydrophobic residues, such as leucine, isoleucine, valine and alanine,[1] and also accumulated in the hydrophobic region of cell membranes.[2-4] In both cases, xenon acts as a modifier of the activity and functional state of transmembrane molecular complexes. More recently, it has been suggested that xenon can reduce the biological function of proteins by forming nanobubbles at or near hydrophobic sites on the protein surface.[5,6]

Studies have been focused on the biologically active properties of xenon used *in vivo*,[7-10] *in vitro*,[11-15] and *in silico*,[16,17] through which detailed data on the anesthetic and analgesic properties of xenon are obtained. However, the experimental *in vivo* approach, where xenon can affect biomolecules by contact with the skin, is completely overlooked. This approach seems quite reasonable, given the good solubility of xenon in hydrophobic media. In addition, it is technically not difficult to provide a high concentration of xenon on the skin area.

How can xenon affect the barrier function of the epidermis and its integrity? How can xenon affect the physiology of deeper skin layers? These questions remain unanswered, and we have not found any mention of it in the scientific literature. It should be taken into account that the physiology and pathophysiology of the skin is very complex, and what the expected bioeffects of xenon are, is difficult to predict. In this regard, at this stage of research on biological properties of xenon in relation to "simple" barrier properties of the skin, we consider it appropriate to use the model of artificial skin analogues, namely, membrane Strat-M™ patches.[18] This approach has successfully proven itself in studies of transdermal diffusion and permeability of a number of compounds.[19-25] Niacinamide, a widely used cosmetic ingredient, was chosen as the permeant. It stabilizes the barrier function of the epidermis, stimulates ceramide synthesis, accelerates differentiation of keratinocytes, smooths wrinkles, and reduces photoinduced and age-related pigmentation in the skin.[26-28] In addition, the laboratory has a well-established protocol for chromatographic analysis of niacinamide.

Materials and Methods

Chromatography for niacinamide

All experiments were performed on a Thermo Scientific™ UltiMate™ 3000 UHPLC system (Thermo Fisher Scientific, Waltham, MA, USA) with a ultraviolet detector. The column used was a Zorbax Eclipse Plus Phenyl-Hexyl stationary phase (Agilent Technologies, Inc., Santa Clara, CA, USA), 150 × 4.6 mm, 3.5 µm.

Buffer solution was prepared by dissolving 3.2 g of ammonium dihydrophosphate (JSC VEKTON, St. Petersburg, Russia) and 250 µL of concentrated phosphoric acid in 1 L of water. The mobile phase was prepared by mixing 980 mL of buffer solution and 20 mL of acetonitrile (PanReac AppliChem GmbH, Darmstadt, Germany). Flow rate was 1.0 mL/min with isocratic elution. The column temperature was set to 30°C. The detection wavelength was set to 210 nm. Injected volume was 20 µL. Standard solution and calibration solutions were prepared by dissolving a dry sample (niacinamide; DSM Nutritional Products Ltd., Basel, Switzerland) of the standard in deionized water.

Chromatography for xenon

A Chromatec-Crystall 5000.1 gas chromatograph (Chromatec, Yoshkar-Ola, Russia) with a thermal conductivity detector was used for the analysis. Sample with xenon (Akela-N Ltd., Moscow, Russia) was placed into the vial, previously weighed

© 2022 Medical Gas Research | Published by Wolters Kluwer - Medknow

together with the lid and the membrane cover. Second weighing was done to determine the mass of the sample in the vial. The vial with the sample was placed in a thermostat (75°C). Two needles with capillaries were inserted into the membrane cover. The first needle was connected to a six-way chromatograph splitter and the gas exiting the vial was blown and accumulated in a calibrated loop (1 mL) of the splitter. The second needle was connected to a vessel containing saturated aqueous NaCl solution (ρ = 1.17 g/mL, t = 20°C), then tap was opened and the solution pumped the air from the vial and xenon released from the sample entered into the chromatograph loop. After that by turning the valve the gas mixture (xenon + air) was injected into the chromatograph for separation and quantification of xenon.

To separate xenon from air a 4 m long packed chromatographic column with NaX sorbent (fraction 60/80; Chromlab, Lyubertsy, Russia) was used. The sequence of the gases leaving the column was following: helium, hydrogen, neon, oxygen + argon, nitrogen, methane, carbon monoxide, krypton, xenon. Helium used as a carrier gas. Column thermostat temperature was set to 80°C. Rate of carrier gas was set to 30 mL/min. The concentrations of the components of the gas mixture were calculated by the method of absolute calibration using samples with known xenon concentration using software package Chromatec Analytic 2.5 (Chromatec).

Preparation of Strat-M™ membranes

Due to high xenon solubility in oils (20 times better than in water),[29,30] it was decided to use the neutral emollient Cetiol® CC (BASF Personal Care and Nutrition GmbH, Monheim, Germany) as xenon solvent that will serve as an efficient source of xenon. Strat-M™ membranes (Merck Millipore, Burlington, MA, USA) were mounted and incubated in three Franz cells (PermeGear, Inc., Hellertown, PA, USA) for 45 minutes at 37°C with a phosphate-buffered saline (PBS)-filled acceptor chamber before the experiment. Xenon-containing niacinamide (1×) solution was prepared ex-temporo. Gas was mixed with 10 mL of the prepared niacinamide solution (5%) in PBS by vigorous shaking it in a 20 mL syringe. The concentration of xenon in PBS was 0.86 ± 0.1 mg/g (n = 3). Niacinamide solution with half xenon content (0.5×) was obtained by preparing 20 mL of niacinamide solution (5%) in PBS from which 10 mL was taken, saturated with xenon, and mixed with the remaining 10 mL of niacinamide xenon-free solution. 1 mL of the solution was placed in the donor chamber of each Franz cell. The sampling volume was 0.4 mL for xenon and 0.4 mL for niacinamide measurements. Samples were collected every hour (up to 8 hours).

Light microscopy

An Amszoom trinocular light microscope (AmScope, Irvine, CA, USA) was used to observe the xenon nucleation on Strat-M™ membranes.

Statistical analysis

Samples with xenon and niacinamide were collected during 8 hours from three separate Franz cells every hour for further use in chromatography analysis. Permeability parameters were derived from the total amount of xenon and niacinamide diffused through a membrane surface area (mg/cm^2) unit per time unit. Results are presented as mean ± standard deviation (SD) ($n \geq 3$). Statistical analysis of the data was performed with one-way analysis of variance followed by Scheffe post hoc test using the Microcal Origin software package (version 8.1; OriginLab Corporation, Northhampton, MA, USA).

Results

Transmembrane diffusion of xenon

The resulting concentration of xenon in Cetiol® CC was 16.01 ± 1.07 mg/g (n = 4). It was shown that xenon diffuses effectively through the membranes (**Figure 1**), and the diffusion rate is comparable with the case when the membrane was not used and the interface was the boundary between Cetiol® CC in the donor chamber and PBS in the acceptor chamber.

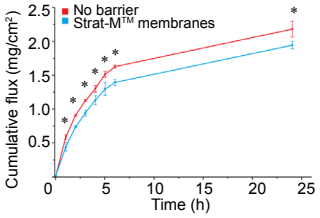

Figure 1: Cumulative xenon flux in the absence of a barrier and through Strat-M™ membranes.

Note: Data are presented as mean ± SD. The experiments were repeated five times. *P < 0.05, no barrier group (n = 5) *vs.* Strat-M™ membranes group (n = 4) (one-way analysis of variance followed by Scheffe *post hoc* test).

Transmembrane diffusion of niacinamide in the presence of xenon

In a transdermal diffusion study of a 5% solution of niacinamide, it was shown that xenon works as an enhancer – it increases the permeation rate of niacinamide across Strat-M™ membranes (**Figure 2A** and **B**). However, the enhancer effect is stronger at lower concentrations of xenon, and only during the first 4 hours from the onset of experiment (**Figure 2C**).

Nucleation of xenon on Strat-M™ membranes

The proposed mechanism of xenon acting as an enhancer is different from the previously described.[31] A possible mechanism of xenon influence on transdermal diffusion of niacinamide is the formation of xenon microbubbles on hydrophobic groups (heterogeneous nucleation). The polyolefin layer of the Strat-M™ membrane contains a combination of lipids (ceramides, cholesterol, free fatty acids and other components) in a specific ratio similar to that found in the human epidermis.[19] These groups may serve as centers for xenon nucleation. We tested the principle possibility of xenon nucleation on Strat-M™ membranes under conditions of maximum PBS saturation with xenon (1×) (**Figure 3**). Placing the Strat-M™ membrane strips in xenon solution, we observed nucleation, in which the bubbles became most distinguishable after half an hour from the moment of immersion.

Discussion

To understand the enhancer effect of xenon on niacinamide diffusion, we propose a simplified model (**Figure 4**) of the three-layer Strat-M™ membrane as a single pore with the narrowest part in the upper region, which mimics the stratum

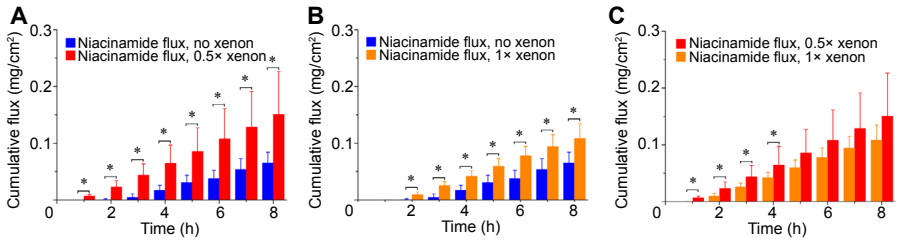

Figure 2: Dose-dependent effect of xenon on transdermal diffusion of niacinamide across Strat-M™ membranes.
Note: (A) Enhancing effect of 0.5× xenon concentration (n = 12) on niacinamide transmembrane flux compared to nicainamide flux without xenon (n = 9). (B) Same as in A, but 1× xenon concentration was used (n = 9). (C) A lower (0.5×) xenon concentration results in a partial increase of xenon properties as an enhancer compared to the maximum 1× xenon concentration. Comparison of the niacinamide accumulation curves for the 1× and 0.5× cases shows that the diffusion of niacinamide for the 0.5× case is enhanced during the first 4 hours. Data are presented as mean ± SD. *P < 0.05 (one-way analysis of variance followed by Scheffe *post hoc* test).

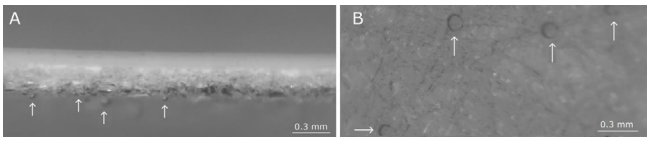

Figure 3: Nucleation of xenon on Strat-M™ membranes.
Note: (A) View from the cut side of the membrane 5 minutes after immersion in phosphate-buffered saline maximally saturated with xenon (1×). (B) View from the dermal side of the membrane 35 minutes after immersion. Arrows indicate forming xenon bubbles. Scale bars: 0.3 mm.

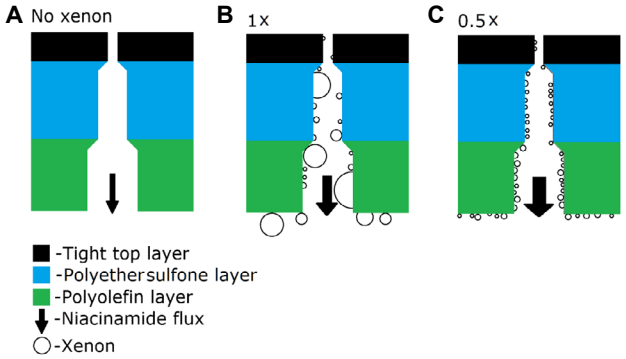

Figure 4: The proposed mechanism of xenon as an enhancer in Strat-M™ membranes.
Note: (A) Niacinamide diffuses freely through the membrane (no xenon). (B) Maximum saturation (1×) xenon nucleation at the internal interfaces accompanied by partial overlapping of niacinamide diffusion pores due to the formation of massive bubbles (the enhancer effect of xenon is weakened). (C) Half saturation (0.5×) xenon nucleation on the hydrophobic parts of the membrane facilitates niacinamide diffusion (xenon is acting as an enhancer).

corneum. Then the pore has an intermediate diameter (representing dermis layer) and the widest part as the lower region of the membrane (representing hypodermis). It is possible that xenon forms microbubbles on the interphase zones of the walls of such a pore. In this case, we can assume partial shielding of the pore surface by "sticking" xenon microbubbles, which fill its roughness. This phenomenon can facilitate the diffusion of niacinamide molecules from the high concentration zone (the donor chamber of Franz cells) to the low in acceptor chamber through the Strat-M™ membrane.

A similar explanation is given in microfluidics research as a superhydrophobic slippage phenomenon, when air microbubbles modify the surface from Wenzel state to Cassie state.[32] For our case this explanation of the xenon enhancing effect is challenged by the fact that there is no fluid flow along the interfaces of micropores but passive diffusion of niacinamide molecules along the concentration gradient. Moreover, the interaction of niacinamide molecules with the inner surface of Strat-M™ membrane micropores to the diffusion process must be taken into account. The intensity of xenon nucleation process inside the pore depends mainly on its concentration. It is quite possible that at maximum concentration of xenon its microbubbles during nucleation may grow in size that becomes comparable with the diameter of the pore in the middle and lower parts of the membrane. Apparently, the amount of dissolved xenon in this zone reaches the level when the formation of such microbubbles becomes possible. In this case, some micropores are blocked by xenon microbubbles and excluded from net transmembrane diffusion of niacinamide.

In our experiments xenon at both used concentrations operates as an enhancer. But, in the case of maximum saturation of PBS with xenon (1×), there may be partial overlapping of large bubbles with already larger diameter pores, leading to a decrease in the total lumen for transmembrane diffusion of niacinamide. In this case, the enhancer effect is less pronounced. Nevertheless, it is possible that overlapping of large pores in the membrane due to xenon nucleation also occurs in 0.5× case at late stages (more than 4 hours from the onset of experiment), and this explains the absence of significant differences in the xenon enhancing effect (**Figure 2C**) for 0.5× and 1× cases, suggesting that it is weakening at the later stages of experiment.

There are some deficiencies and limitations in this study. In particular, the donor chamber of the Franz cell can not be considered as an infinite xenon source due to its rapid diffusion into the acceptor part. Therefore, we had to limit the duration of our experiments to 8 hours maximum. The light microscopy allowed us to visualize the nucleation of xenon in the form of large bubbles on the dermal surface of the Strat-M™ membrane, but not the forming microbubbles in the layers of the membrane, what would be the direct proof of our hypothesis. It should also be noted that Strat-M™ membranes are a simplified analogues of the skin. They possess no metabolic activity, and have different chemical composition. Direct extrapolation of observed enhancing activity of xenon on native skin preparations should be done with caution.

The obtained data suggest that xenon can be considered as a promising transdermal enhancer with a new mechanism of action. However, the optimal concentration of xenon, at which its properties as an enhancer are manifested to the maximum extent, remains unknown. The question whether xenon will

show its ability to act as an enhancer in case of using other permeants, as well as the scenario of utilizing native skin preparations, heat separated epidermis, etc., remains unanswered and needs further research.

Author contributions
Conception of the work, experiment design, literature search: AV. Data acquisition, experiment design, data analysis, literature search, manuscript preparation: EP. Both the authors read and approved the final version of the manuscript for publication.

Conflicts of interest
Xenon Diffusion is in the patent pending process.

Financial support
This work was supported by the Xenon Skincare International, Inc. (East Stroudsburg, PA, USA), represented by Dr. Mikhail Artamonov. Neither the experimental design nor the results of this work were affected by the funder.

Copyright license agreement
The Copyright License Agreement has been signed by all authors before publication.

Data sharing statement
Individual participant data that underlie the results reported in this article, after deidentification (text, tables, figures, and appendices). Study protocol and informed consent form will be available immediately following publication, without end date. Results will be disseminated through presentations at scientific meetings and/or by publication in a peer-reviewed journal. Anonymized trial data will be available indefinitely at www.figshare.com.

Plagiarism check
Checked twice by iThenticate.

Peer review
Externally peer reviewed.

Open access statement
This is an open access journal, and articles are distributed under the terms of the Creative Commons Attribution-NonCommercial-ShareAlike 4.0 License, which allows others to remix, tweak, and build upon the work non-commercially, as long as appropriate credit is given and the new creations are licensed under the identical terms.

References

1. Prangé T, Schiltz M, Pernot L, et al. Exploring hydrophobic sites in proteins with xenon or krypton. *Proteins*. 1998;30:61-73.
2. Booker RD, Sum AK. Biophysical changes induced by xenon on phospholipid bilayers. *Biochim Biophys Act*a. 2013;1828:1347-1356.
3. Weinrich M, Worcester DL. Xenon and other volatile anesthetics change domain structure in model lipid raft membranes. *J Phys Chem B*. 2013;117:16141-16147.
4. Reyes-Figueroa AD, Karttunen M, Ruiz-Suárez JC. Cholesterol sequestration by xenon nano bubbles leads to lipid raft destabilization. *Soft Matter*. 2020;16:9655-9661.
5. Zhang L, Zhang Y, Cheng J, et al. Inert gas deactivates protein activity by aggregation. *Sci Rep*. 2017;7:10176.
6. Theodorakis PE, Che Z. Surface nanobubbles: Theory, simulation, and experiment. A review. *Adv Colloid Interface Sci.* 2019;272:101995.
7. Campos-Pires R, Hirnet T, Valeo F, et al. Xenon improves long-term cognitive function, reduces neuronal loss and chronic neuroinflammation, and improves survival after traumatic brain injury in mice. *Br J Anaesth*. 2019;123:60-73.
8. Koziakova M, Harris K, Edge CJ, Franks NP, White IL, Dickinson R. Noble gas neuroprotection: xenon and argon protect against hypoxic-ischaemic injury in rat hippocampus in vitro via distinct mechanisms. *Br J Anaesth*. 2019;123:601-609.
9. Yin X, Moody MR, Hebert V, et al. Oral delivery of xenon for cardiovascular protection. *Sci Rep*. 2019;9:14035.
10. Zhu Y, Mosko JJ, Chidekel A, Wolfson MR, Shaffer TH. Effects of xenon gas on human airway epithelial cells during hyperoxia and hypothermia. *J Neonatal Perinatal Med.* 2020;13:469-476.
11. Hantal G, Fábián B, Sega M, Jójárt B, Jedlovszky P. Effect of general anesthetics on the properties of lipid membranes of various compositions. *Biochim Biophys Acta Biomembr.* 2019;1861:594-609.
12. Petrov E, Menon G, Rohde PR, Battle AR, Martinac B, Solioz M. Xenon-inhibition of the MscL mechano-sensitive channel and the CopB copper ATPase under different conditions suggests direct effects on these proteins. *PLoS One*. 2018;13:e0198110.
13. Pavel MA, Petersen EN, Wang H, Lerner RA, Hansen SB. Studies on the mechanism of general anesthesia. *Proc Natl Acad Sci U S A*. 2020;117:13757-13766.
14. Bürge M, Kratzer S, Mattusch C, et al. The anaesthetic xenon partially restores an amyloid beta-induced impairment in murine hippocampal synaptic plasticity. *Neuropharmacology.* 2019;151:21-32.
15. Roose BW, Zemerov SD, Dmochowski IJ. Xenon-protein interactions: characterization by X-ray crystallography and hyper-CEST NMR. *Methods Enzymol.* 2018;602:249-272.
16. Smith J, Zadeh Haghighi H, Salahub D, Simon C. Radical pairs may play a role in xenon-induced general anesthesia. *Sci Rep.* 2021;11:6287.
17. Winkler DA, Warden AC, Prangé T, et al. Massive in silico study of noble gas binding to the structural proteome. *J Chem Inf Model.* 2019;59:4844-4854.
18. Neupane R, Boddu SHS, Renukuntla J, Babu RJ, Tiwari AK. Alternatives to biological skin in permeation studies: current trends and possibilities. *Pharmaceutics*. 2020;12:152.
19. Haq A, Goodyear B, Ameen D, Joshi V, Michniak-Kohn B. Strat-M® synthetic membrane: permeability comparison to human cadaver skin. *Int J Pharm.* 2018;547:432-437.
20. Bolla PK, Clark BA, Juluri A, Cheruvu HS, Renukuntla J. Evaluation of formulation parameters on permeation of ibuprofen from topical formulations using Strat-M(®) membrane. *Pharmaceutics*. 2020;12:151.
21. Kuznetsova EG, Kuryleva OM, Salomatina LA, Belov VY, Sevastianov VI. The cyclosporine transdermal transfer possibility study on model systems. *Russ J Transplantol Artif Organs*. 2019;21:135-141.
22. Uchida T, Kadhum WR, Kanai S, Todo H, Oshizaka T, Sugibayashi K. Prediction of skin permeation by chemical compounds using the artificial membrane, Strat-M™. *Eur J Pharm Sci.* 2015;67:113-118.
23. Kaur L, Singh K, Paul S, Singh S, Singh S, Jain SK. A mechanistic study to determine the structural similarities between artificial membrane Strat-M™ and biological membranes and its application to carry out skin permeation study of amphotericin B nanoformulations. *AAPS PharmSciTech*. 2018;19:1606-1624.
24. Arce FJ, Asano N, See GL, Itakura S, Todo H, Sugibayashi K. Usefulness of artificial membrane, Strat-M(®), in the assessment of drug permeation from complex vehicles in finite dose conditions. *Pharmaceutics.* 2020;12:173.
25. Haq A, Dorrani M, Goodyear B, Joshi V, Michniak-Kohn B. Membrane properties for permeability testing: Skin versus synthetic membranes. *Int J Pharm*. 2018;539:58-64.
26. Campiche R, Curpen SJ, Lutchmanen-Kolanthan V, et al. Pigmentation effects of blue light irradiation on skin and how to protect against them. *Int J Cosmet Sci.* 2020;42:399-406.
27. Gehring W. Nicotinic acid/niacinamide and the skin. *J Cosmet Dermatol*. 2004;3:88-93.
28. Voegeli R, Guneri D, Cherel M, Summers B, Lane ME, Rawlings AV. Topical niacinamide enhances hydrophobicity and resilience of corneocyte envelopes on different facial locations. *Int J Cosmet Sci.* 2020;42:632-636.
29. Weathersby PK, Homer LD. Solubility of inert gases in biological fluids and tissues: a review. *Undersea Biomed Res.* 1980;7:277-296.
30. Steward A, Allott PR, Cowles AL, Mapleson WW. Solubility coefficients for inhaled anaesthetics for water, oil and biological media. *Br J Anaesth*. 1973;45:282-293.
31. Williams AC, Barry BW. Penetration enhancers. *Adv Drug Deliv Rev.* 2004;56:603-618.
32. Roach P, Shirtcliffe NJ, Newton MI. Progess in superhydrophobic surface development. *Soft Matter*. 2008;4:224-240.

Date of submission: April 30, 2021
Date of decision: May 8, 2021
Date of acceptance: August 21, 2021
Date of web publication: August 30, 2021